Saline groundwater evolution in Luanhe River Delta, China since Holocene: hydrochemical, isotopic and sedimentary evidence

Xianzhang Dang[a, b, c], Maosheng Gao[b, d], Zhang Wen[a], Guohua Hou[b, d], Hamza Jakada[e], Daniel Ayejoto[a], Qiming Sun[a, b,c]

[a]School of Environmental Studies, China University of Geosciences, 388 Lumo Rd, Wuhan, 430074, China

[b]Qingdao Institute of Marine Geology, CGS, Qingdao, 266071, China

[c]Chinese Academy of Geological Sciences, Beijing, 100037, China

[d]Laboratory for Marine Geology, Pilot National Laboratory for Marine Science and Technology, Qingdao, 266071, China

[e]Department of Civil Engineering, Baze University Abuja, Nigeria

Correspondence to: Maosheng Gao (gaomsh66@sohu.com), Zhang Wen (wenz@cug.edu.cn)

Abstract

Since the Quaternary Period, palaeo-seawater intrusions have been suggested to explain the observed saline groundwater that extends far inland in coastal zones. The Luanhe River Delta (northwest coast of Bohai Sea, China) is characterized by the distribution of saline, brine, brackish and fresh groundwater, from coastline to inland, with a wide range of total dissolved solids (TDS) between 0.38-125.9 g/L. Meanwhile, previous studies have revealed that this area was significantly affected by Holocene marine transgression. In this study, we used hydrochemical, isotopic, and sedimentological methods to investigate groundwater salinization processes in the Luanhe River Delta and its links to the palaeo-environmental settings. The isotopic results (^{2}H, ^{18}O, ^{14}C) facilitate the distinciton between old and new groundwater recharge.~~show that deep confined groundwater was recharged during the Late Pleistocene cold period, shallow saline and brine groundwater was recharged during the warm Holocene period, and shallow brackish and fresh groundwater was mainly recharged by surface water. The results of hydro-geochemical modeling (PHREEQC) suggest that the salty sources of salinization are seawater and concentrated saline water (formed after evaporation of seawater).~~ Results of the hydro-chemical analysis using PHREEQC indicate that the origin of salt in saline and brine groundwater is from a marine source. The ^{18}O-Cl relationship diagram yields three end-member mixing of groundwater with wo mixing scenarios suggested to explain the freshening and salinization processes in study area. ~~shows that saline and brine groundwater are formed by three end-member mixings (seawater, concentrated saline water and, fresh groundwater). In contrast, brackish~~

~~groundwater is formed after the wash-out of saline groundwater by surface water. Using palaeo-environmental data from sediments, we found that palaeo-seawater intrusion during the Holocene marine transgression was the primary cause of groundwater salinization in the study region. Seawater was found to evaporate in the lagoon area during the progradation of the Luanhe River Delta; the resulting concentrated saline water infiltrated into the aquifer, eventually forming brine groundwater due to salinity accumulation. Surface water recharge and irrigation, on the other side, would gradually flush the delta plain's saline groundwater. This study provides a better understanding of saline groundwater evolution in other similar coastal zones.~~ When interpreted with data from palaeo-environmental sediments, we found that groundwater salinization may have occurred since the Holocene marine transgression. The brine is characterized by radiocarbon activities of ~50 to 85 pMC and relatively depleted stable isotopes, which is associated with seawater evaporation in the ancient lagoon during delta progradation, as well as mixing with deeper fresh groundwater which probably was recharged in cold late Pleistocene. As for the brackish and fresh groundwater, they are characterized by river-like stable isotope values where high radiocarbon activities (74.3 to 105.9 pMC) were formed after the wash-out of salinized aquifer by surface water in the delta plain."

Introduction

It is estimated that 20-40% of the world's population lives in coastal areas. (Small and Nicholls, 2003; Martinez et al., 2007; UN Atlas, 2010). Groundwater is the primary source of fresh water in this region (Cary et al., 2015). However, groundwater salinization poses a significant threat to everyday living and development activities (Cost Environment Action 621, 2005; de Montety et al., 2008). In recent decades, groundwater salinization in coastal zones are widely concerned and studied. On the one hand, seawater intrusion due to groundwater pumping is a vital salinization process in the coastal aquifer (Reilly and Goodman, 1985; Werner, 2010, 2013; Han and Currell, 2018). On the other hand, groundwater salinization caused by the palaeo-seawater intrusion, in response to the Quaternary changes in global sea-level, has been reported in many coastal zones worldwide (Edmunds, 2001; Akouvi, 2008; Santucci et al., 2016, Larsen et al., 2017).

Coastal aquifers are linked to the ocean and continental hydrological cycle (Ferguson and Gleeson, 2012), both of which are influenced by natural and human-induced change (Jiao and Post, 2019). There is a steady-state seawater-freshwater interface under the natural state that extends inland from the coastal line (Costall et al., 2020). ~~Overexploitation of groundwater locally decreases the land groundwater head, shifting the interface downstream and causing salinization of the freshwater aquifer, which is a phenomenon influenced by human factors (Werner et al., 2013). Since the Quaternary period, however, sea-level fluctuations on geological timescales~~ have caused the interface to change, allowing seawater intrusion during transgression events and freshwater flushing during glacial low sea-level periods, which are evident in hydrochemical characteristics of groundwater in coastal aquifers ~~are the primary factors influencing groundwater quality in coastal areas~~ (Kooi et al., 2000; Sanford, 2010; Aquilina et al., 2015; Lee et al., 2016). In addition, the hypersaline groundwater found in coastal zones, particularly brine groundwater with a salinity of 2-4 times that of seawater, cannot be explained solely by using a seawater intrusion model (Sola et al., 2014, Han et al., 2020), and palaeoenvironment settings must be taken into consideration (Van Engelen et al., 2019). Some studies, for example, attribute the presence of brine in Mediterranean countries to the evaporation of seawater in the lagoon system during the Holocene transgression (Giambastiani et al., 2013, Vallejos et al., 2018).

The Bohai Sea of northern China was affected by Late Pleistocene transgressive-regressive cycles, which caused various salinity palaeo-saltwater intrusion along the coastal aquifers (Du et al., 2015; Li et al., 2017). Several studies have applied geochemical methods to elucidate the origin of saline groundwater and the salinization processes under anthropogenic influence, including induced mixing brine water from adjacent aquifers caused by groundwater overexploitation in Laizhou Bay (Han et al., 2011, 2014; Liu et al., 2017; Qi et al., 2019). However, the association between groundwater salinization (especially brine formation) and palaeoenvironmental implications are still not clear. Thus, this study applies a range of chemical, isotopic and sedimentary indicators to examine the Luanhe River Delta (situated along the northwestern coast of Bohai Sea) to elucidate the groundwater salinization processes in relation to recharge, salt source, mixing behavior and palaeogeographic evolution. The overall goal is to understand the groundwater evolutionary pattern influenced by transgression/regression events in geologic time. The findings will be significant to aquifer remediation activities in the region as well as other similar sedimentary environments around the world.

~~Deceleration of sea-level rise since the mid-Holocene has resulted in the formation of global deltas (Stanley and Warne, 1994). Meanwhile, various salinity palaeo-saltwater has been found in these delta aquifers at distances up to 100 km from current coastlines (Larsen et al., 2017). Hydrogeochemical, isotopic methods (Wang and Jiao, 2012; Geriesh et al., 2015; Tran et al, 2020) and numerical simulations (Tran et al., 2012; Delsman et al., 2014; van Engelen et al., 2018) were used to illustrate the origin of the inland saline groundwater. Few studies examine the response of saline groundwater evolution to the palaeoenvironment development. The Luanhe River Delta, situated on the northwest coast of Bohai Sea, is an independently developed Holocene coastal delta, with fresh, brackish, saline, and brine groundwater distributed from land to sea in the shallow aquifer (Dang et al., 2020).~~

~~In this study, we used a range of chemical and isotopic indicators to determine the salinity sources and recharge condition. Using sedimentary evidence from the reported cores, we have been able to identify groundwater salinization processes and the genesis of brine which had been subjected to complex climate, geomorphological and hydrological evolution. This research can be used to better understand saline groundwater evolution in other coastal zones and, as a result, better manage~~

~~groundwater resources.~~

2 Background of the study area

The study area is located in northeastern Hebei Province, China, on the west coast of Bohai (Fig. 1a). The study area consists of alluvial fan and coastal delta, bounded by Holocene maximum transgression line (Xue et al., 2016). The delta area can be further divided into two parts: old delta between the Douhe River and the Suhe River, the new delta between the Suhe River and the modern Luanhe River (He et al., 2020). The geomorphology of the study area is inclined to the south and southwest with a slope of about 0.04-2‰. The temperate monsoon climate affects the average annual temperature of 12.5°C and annual rainfall of 601 mm (1956-2010), with 80% of the annual rainfall occurring between July and September.

2.1 Hydrogeology

The thickness of Quaternary sediments in the study area is about 400-500 m. According to the lithology and hydrogeological characteristics, the Quaternary aquifers are made up of four distinct aquifers (Fig. 1b): the First Holocene aquifer (Q_4) is a phreatic or semi-confined aquifer with a bottom depth of 15-30 m and is primarily composed of fine sand and slit, involving fresh, brackish, saline and brine groundwater (Dang et al., 2020). The second Late Pleistocene aquifer (Q_3), the third Middle Pleistocene aquifer (Q_2), and the fourth Early Pleistocene aquifer (Q_1), with bottom depths of 120-170 m, 250-350 m, and 350-550 m, respectively. They have confined aquifers primarily made up of medium sand and gravel (Niu et al., 2019). The first aquifer is mainly recharged by meteoric precipitation and lateral infiltration of surface water (Li et al., 2013). In the alluvial fan areas, the groundwater from the first aquifer is widely extracted for irrigation. The largest salt farm in north China, the Daqinghe Salt Farm, uses shallow brine groundwater for salt production in the delta area, where agricultural activities are small. Except for the area of alluvial fan, the circulation between phreatic and confined aquifers is weak. The deep groundwater in second, third, and fourth aquifers are mainly recharged by a surrounding mountain range and mainly discharged by human pumping (Ma et al., 2014).

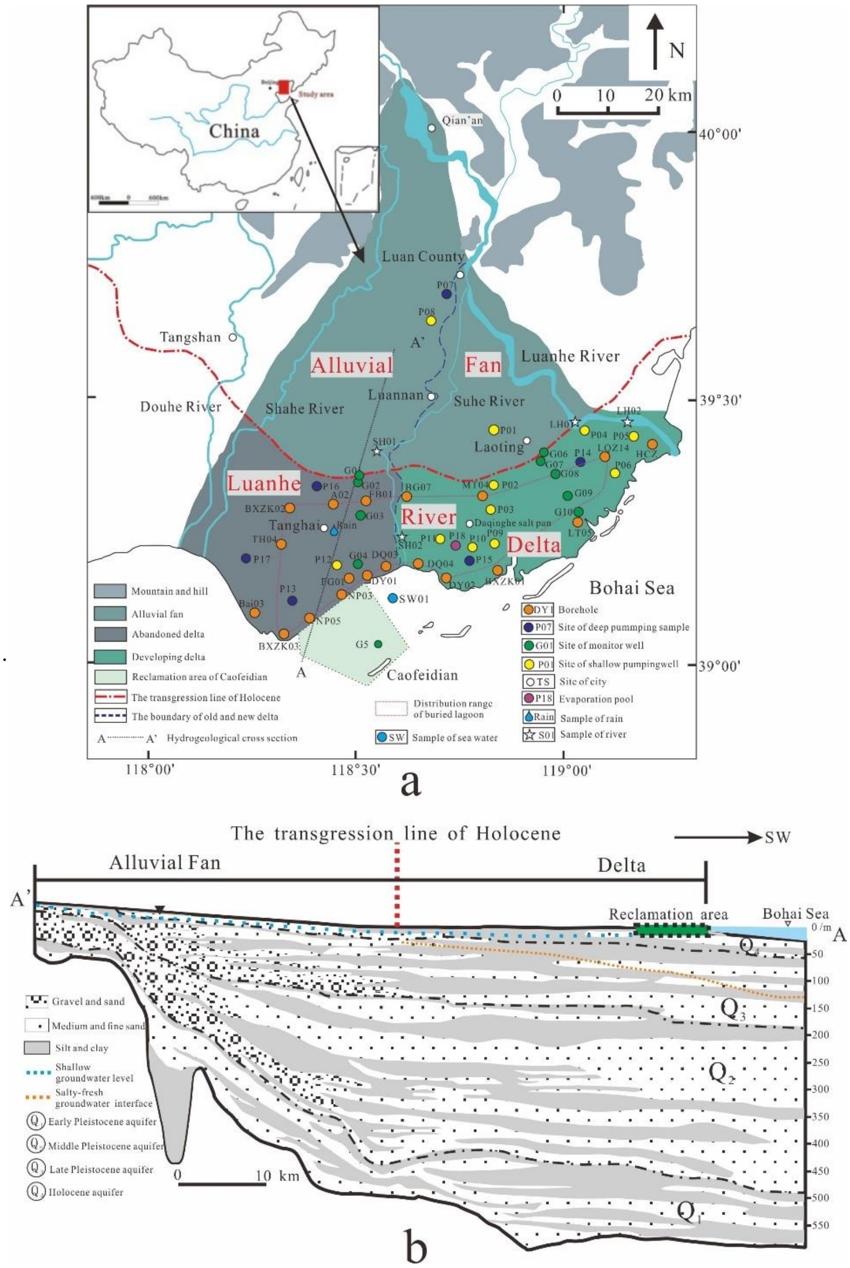

Fig. 1. (a) Location map of study area. Also shown are the sampling site and published cores in the Luanhe River Delta. Cores LT05, HCZ, BXZK01, BXZK02 and BXZK03 were cited from He et al. (2020); Cores NP05, NP03, DY01, DQ03, DQ04, DY02, MT04, BG07, FB01, A02 and TH04 were cited from Xu et al. (2020); Core LQZ04 was cited from Cheng et al. (2020); Core FG01 was cited from Xu et al. (2011); Core Bai03 was cited from Li and Wang. (1983); Core HCZ was cited from Peng et al. (1981). (b) Hydrogeological cross-section (A-A' in Fig. 1a) of study area, modified by Ma et al., 2014.

~~2.2 Marine transgression history~~

~~During the Quaternary period, there were several times of marine transgression-regression events in the Bohai basin (Wang et al., 1981, Xu et al., 2018), which were significantly influenced by neotectonics (Liu et al., 2016). The published cores show that the Holocene marine or paralic deposits are widely involved in the study area (Peng et al., 1981; Li et al., 1982; Xu et al., 2020). Furthermore, the MIS5 marine deposits are observed in core FG01 at 80-105 m (Xu et al., 2011) and core Bai03 at 33-46 m (Li and Wang, 1983), both of which are close to the shoreline (Fig. 1a). Except for the sediments at a depth of 40 m in core FG01 (Xu et al., 2011), few studies report MIS3 marine deposits in the study area. Moreover, the inland core BXZK02 (Fig. 1a) is clearly lacking MIS3 marine deposit, provided that MIS5 marine deposits are involved at a depth of 23.3-27.2 m, but the upper sediments were fluvial deposit (about 90-30 ka B.P. age) at 13-23 m deep (He et al., 2020). In conclusion, seawater invaded the study area during Holocene marine transgression; MIS3 and MIS5 marine transgression once reached this area, and seawater may have flooded the land area during MIS5 marine~~

~~transgression, however, MIS3 marine transgression was less dominant and may not have reached the modern land area.~~

2.~~3~~2 Sedimentary evolution since the Late Pleistocene

Previous studies have shown that in the study region, the interface of salt-fresh groundwater gradually deepens from land (depth of ~ -5 m) to sea(depth of ~ -100 m), as shown in Fig. 1b, with salt groundwater primarily occurring in the first aquifer of the delta area (Li et al., 2013; Ma et al., 2014). According to stratigraphic transect along the present coastline (Fig. 2), the series stratigraphic architecture of the first aquifer consists of Late Pleistocene continental facies - Holocene marine facies - Holocene~~ sea-land transition facies (~~delta facies~~)~~ - modern continental facies or artificial fill, indicating that the sediments of the first aquifer had been deposited from lowstand continental accumulation to marine transgression and high stand progradation since the Late Pleistocene.

The seawater had not reached the modern coastline from the Last Glacial Maximum to the early Holocene (about 30-9 ka B.P.). The Luanhe alluvial fan was an activity in this period (He et al., 2020). Since about 9000 a B.P., the Holocene marine transgression had approached the present coastline (Xu et al., 2020), and Holocene marine sediments developed under the sea-level rising condition from 9-7 ka B.P. The Holocene marine transgression had reached its maximum inland area 20 km from the modern coastline until about 7 ka BP (Gao et al., 1981; Peng et al., 1981; Xue, 2014, 2016) (Fig. 1 transgression line of Holocene), the accumulation of highstand prograding delta on top of Holocene marine strata, together with the artificial fill formed the modern coastal plain. In addition, lagoons are important components of the Luanhe River Delta (Feng and zhang, 1998). According to the records of lagoon facies in the published cores in this region, the approximate distribution range of buried lagoon is shown as a purple dashed line in Fig. 1a.

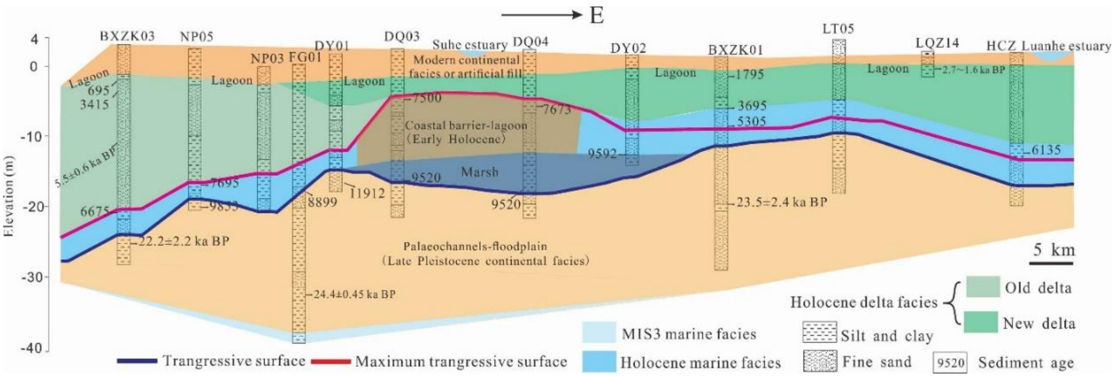

Fig.2 Stratigraphic transect along the present coastline of Luanhe River Delta, modified from He et al.,2020.

3 Methods

In total, 45 water samples were collected from the Luanhe River Delta, including 38 groundwater samples, 5 surface water samples, 1 local rain water and 1 Bohai seawater samples, during 4 sampling campaigns from October 2016 to June 2020. Groundwater samples were divided into shallow groundwater samples and deep groundwater samples, which were pumped from unconfined aquifer and confined aquifer respectively. Surface water includes 2 Suhe River water samples and 2 Luanhe River water samples. Due to artificial fill that has modified the coastal landscape, it was difficult to locate the modern lagoon environment. However, during the investigation, it was found that the ~~Daqingher~~ Daqinghe salt farm in this area extracts seawater into the evaporation pond. The mixture of seawater and meteoric water is subject to evaporation to form concentrated saline water (CSW) in the pond, which is similar to the formation of CSW in a coastal lagoon (Stumpp et al., 2014). Thus, 1CSW (P18 sample) in the evaporation pond was collected.

Water types were classified according to Zhou (2013): freshwater (TDS < 1 g/L), brackish water (TDS = 1 to 3 g/L), saline water (TDS = 3 to 50 g/L), and brine (TDS > 50 g/L). Groundwater sampling depths and pH values were measured on site using CDT-divers. The concentrations of K^{+}, Na^{+}, Ca^{2+}, Mg^{2+}, and Br^{-} ion were measured using inductively coupled plasma analysis (ICAP-7400), while SO_4^{2-} and Cl^{-} ions were determined using ion chromatography (ICS-600). The HCO_3^{-} concentrations of samples were measured using titration. The hydrochemical data are listed in Table S1(see Supplement). The stable isotope concentrations (δ D, δ ^{18}O) of the water samples (including G02-10, G06-10, G03-05, G04-40, G05-10, G05-46, G07-27, P07-20, P08-30, P09-30, P10-30, P11-20, P12-40 P14-15, P07-100, P13-200, P14-300, P15-150, P16-100, P17-200, P18, LH01, LH02, SH01, SH02, SW01, R1) were tested at the Experimental & Testing Center of Marine Geology, Ministry of Natural Resource, China, using High Temperature Pyrolysis-Isotope Ratio Mass Spectrometry. The values of δ ^{18}O and δ D were calculated with respect to the Vienna Standard Mean Ocean Water (VSMOW), and the uncertainty for δ D and δ ^{18}O are ±1.0‰ and ±0.2‰, respectively. The radioisotope (AMS ^{14}C) of groundwater samples (P14-300, P15-150, and P16-100) were measured at the Pilot National Laboratory for Marine Science and Technology. Stable isotopes (δ D, δ ^{18}O, ^{13}C) and radioisotope of groundwater samples (G10-10, G03-20, G04-15, G05-30, G06-15, G07-15, G08-15, G08-40, G09-15, G09-40, G10-10, G10-30) were analyzed at the Beta Analytic TESTING LABORATORY, where the

$\delta^{18}O$ and δD values were also calculated with respect to VSMOW, and the uncertainty for δD and $\delta^{18}O$ are listed in Table S1. The ~~age of groundwater~~ ^{14}C age of groundwater was calculated using the following equation: ~~$t = -8267 \cdot \ln\left(a_t{}^{14}C / q - a_0{}^{14}C\right)$~~ $t = -8267 \cdot \ln\left(a_t{}^{14}C/q \cdot a_0{}^{14}C\right)$ (Clark and Fritz, 1997), where t is ~~the residence time of groundwater in a B.P.~~ radiocarbon ages in years Before Present (a B.P.); $a_t{}^{14}C$ is the measured ^{14}C activity in % of modern carbon (pMC); $a_0{}^{14}C$ is the modern ^{14}C activity of soil derived; q is a corrective factor, the corrective factor accounts for the dissolution of calcite, which is assumed to be free of ^{14}C and, therefore, dilutes the initial ^{14}C activity of aqueous DIC in recharged water. The results of ^{13}C, ^{14}C and the uncorrected residence times are listed in Table S2.

4 Results

4.1 Hydrochemistry

Except for P13-200 (TDS=1.617 g/L, which is brackish water), all the deep groundwater samples in the study region are freshwater. Deep groundwater hydrochemical forms shift from Ca-HCO_3 to Na-HCO_3 as it moves from land to sea (Fig. 3). For shallow aquifer, the horizontal interface of salt-fresh groundwater corresponds better with the maximum Holocene transgression line (see Fig. 1a). The Ca-HCO_3 type of shallow fresh groundwater is primarily distributed in the alluvial fan region. The brackish and low TDS saline groundwater, which vary from Ca-HCO_3, Na-HCO_3, and Na-Cl types, are mainly contained in the upper aquifer (depth of 0-15 m) of delta area, while the lower part (depth of 20–40 m) is Na-Cl type of saline and brine groundwater with high TDS. Moreover, for horizontal distribution of salinity, the groundwater TDS tends to decrease from west to east, such as the TDS of saline and brine groundwater TDS generally range from 16.57–125.97 g L^{-1} in old delta (western delta), while 3.26–52.48 g L^{-1} in the new delta (eastern delta).

~~Fresh, brackish, saline, and brine water are all forms of shallow groundwater (Table 1), and the horizontal interface of salt-fresh groundwater corresponds better with the maximum Holocene transgression line (see Fig. 1a). The Ca-HCO_3-type of shallow fresh groundwater is primarily distributed in the alluvial fan region, and the brackish, saline and brine groundwater are almost exclusively sampled from the delta area. The hydrochemical type of brackish water is complex, including Ca-HCO3, Na-HCO_3, and Na-Cl types, while the saline and brine is single Na-Cl type.~~

~~For shallow aquifer, vertically, the upper part (depth of 0-15 m) mainly contains brackish and low TDS saline groundwater, while the lower part (depth of 20-40 m) is saline and brine groundwater with high TDS. Moreover, for horizontal distribution of salinity, the groundwater TDS tends to decrease from west to east, such as the TDS of saline and brine groundwater TDS generally range from 16.57-115.75 g/L in old delta (western delta), while 3.26-52.48 g/L in the new delta (eastern delta).~~

Table S1 Hydrochemical and stable isotopic data from water samples in study area.

Water	Position	Site	Label	Depth(m)	ρ(mg/L) K^+	Na^+	Ca^{2+}	Mg^{2+}	Cl^-	SO_4^{2-}	HCO_3^-	Br^-	TDS (g/L)	pH	δ D(‰, VSMOW)	δ ^{18}O(‰, VSMOW)	Uncertainty ‰ δ D	δ ^{18}O
Shallow groundwater:																		
Fresh	Old delta	G01	G01-10	10.00	21.22	14.11	43.34	17.65	19.52	21.48	246.18		0.384	7.60	-58.9	-8.2	±0.39	±0.04
		G02	G02-10	10.00	2.39	73.33	127.27	55.26	79.74	184.82	451.77		0.975	7.32	-44.1	-8.0	±1	±0.2
	Alluvial fan	P01	P01-15	15.00	3.01	64.53	171.10	67.88	173.94	133.59	410.34		1.159	8.42				
		P07	P07-20	20.00	0.973	32.2	144	18.2	64.5	116	199	0.074	0.575	7.78	-57.1	-7.5	±1	±0.2
		P08	P08-30	30.00	1.142	13.3	53.7	16.1	14.0	23.5	151	0.037	0.384	8.20	-58.8	-7.9	±1	±0.2
Brackish	New delta	G06	G06-15	10.00	5.17	209	110	66.4	391	204	338	1.06	1.324	7.59	-59.1	-8.2	±0.37	±0.08
		G08	G08-15	10.00	35.6	666	136	127	1087	415	374	4.38	2.841	7.84	-52.6	-7.3	±0.24	±0.09
		G07	G07-15	15.00	9.70	582.73	229.08	110.97	953.31	457.90	448.50		2.792	7.62	-54.2	-6.5	±0.14	±0.09
		P02	P02-20	20.00	1.99	153.60	164.13	79.93	232.34	226.83	509.28		1.606	8.51				
		P05	P05-20	20.00	56.12	310.82	207.78	112.98	397.58	394.48	686.07		2.584	8.39				
		P14	P14-15	15.00	37.60	811.00	143.00	137.00	1357.00	428.00	398.00	3.94	3.312	7.89	-52.9	-7.5	±1	±0.2
		P06	P06-20	20.00	19.03	532.42	41.36	26.15	435.29	142.11	593.62		1.987	8.34				
Saline	Old delta	G03	G03-5	5.00	162.80	4558.4	336.08	698.13	7949.85	1388.5	1476.45		16.57	6.98	-39.8	-6.7	±1	±0.2
		G04	G04-15	15.00	194.47	13502.	559.29	1725.67	25215.25	3565.6	1034.50		45.797	7.25	-51.2	-6.5	±0.54	±0.07
		G05	G05-10	10.00	200.73	5167.9	337.58	640.08	9113.11	2208.2	432.13		18.099	7.45	-29.8	-4.9	±1	±0.2
			G05-20	20.00	185	5414	291	673	9223	1803	646	38.7	18.235	7.41				
			G05-46	46.00	229.51	6743.2	278.53	824.20	12432.88	1700.9	995.21		23.205	7.44	-25.6	-4.1	±1	±0.2
	New delta	G07	G07-27	27.00	27.11	2043.8	305.71	198.94	3650.06	570.62	350.29		7.147	7.32	-64.6	-8.7	±1	±0.2
		G08	G08-40	40.00	66.31	7371.3	1217.2	1028.62	15073.12	2039.9	376.48		27.173	6.95	-46.2	-5.4	±0.26	±0.07
		G09	G09-15	15.00	27.07	1121.8	236.66	172.54	1885.99	406.47	576.18		4.426	7.2	-45.3	-5.7	±0.55	±0.06
			G09-40	40.00	184.61	11882.	539.23	1557.19	22669.53	2900.7	608.91		40.342	6.77	-39.4	-5.2	±0.45	±0.08
		G10	G10-10	10.00	294.60	9221.2	354.32	1181.33	16220.80	2683.1	674.39		30.629	7.11	-31.4	-4.0	±0.56	±0.05
		P03	P03-20	20.00	16.09	285.29	432.17	202.41	682.71	1139.6	314.65		3.258	7.24				
		P04	P04-30	30.00	50.98	1103.4	133.29	135.89	1775.19	258.68	548.21		5.056	8.38				
		P09	P09-30	30.00	314	12267	408	1469	21909	2730	543	88.8	39.64	7.19	-37.7	-4.9	±1	±0.2
		P10	P10-30	30.00	159	13833	744	2153	26270	3725	586	114	47.47	6.93	-27.7	-3.9	±1	±0.2
		P11	P11-20	20.00	280	15377	707	2147	29689	3542	404	119	52.146	6.90	-26.3	-2.7	±1	±0.2
Brine	Old delta	G03	G03-20	20.00	545.21	25182.	948.30	3245.41	45835.43	4308.9	622.01		80.688	6.65	-27.8	-3.2	±0.22	±0.14
			G03-30	30.00	489	23365	776	3073	42871	4383	525	198	75.48	6.93				
		G04	G04-40	40.00	159.98	23056.	1253.7	3507.54	48229.65	4450.4	667.84		81.325	6.7	-43.1	-6.4	±1	±0.2
		P12	P12-40	40.00	836	39463	759	4695	70961	8518	489	254	125.975	6.68	-36.5	-4.7	±1	±0.2
	New delta	G10	G10-30	30.00	449.23	15416.	437.65	1996.27	29889.91	3358.7	933.01	97.4	52.482	6.98	-22.5	-2.1	±0.22	±0.07
Deep groundwater:																		
Brackish	Old delta	P13	P13-200	200.00	1.34	452	40.2	31.5	417	120	555	2.01	1.617	7.66	-70.0	-9.1	±1	±0.2
Fresh	Alluvial fan	P07	P07-100	100.00	1.143	19.8	45.2	12.8	12.1	13.4	163	0.036	0.267	8.29	-57.1	-7.6	±1	±0.2
	New delta	P14	P14-300	300.00	0.388	104.0	17.1	3.38	29.0	20.4	205	0.10	0.379	8.14	-71.3	-9.8	±1	±0.2
		P15	P15-150	150.00	0.540	116	14.5	3.40	35.0	45.2	266	0.14	0.481	7.65	-70.4	-9.0	±1	±0.2
	Old delta	P17	P17-200	200.00	0.286	144	6.29	1.61	24.5	72.0	241	0.089	0.489	8.48	-75.5	-8.6	±1	±0.2
		P16	P16-100	100.00	0.355	42.6	41.8	12.5	5.29	28.4	235	0.021	0.365	8.13	-67.8	-9.0	±1	±0.2
Surface water:																		
Fresh	New delta	LH01	LH01		6.16	27.25	68.93	25.67	35.41	123.53	199.70		0.492	7.95	-53.5	-8.4	±1	±0.2
		LH02	LH02		6.28	27.96	68.65	26.05	36.84	124.71	199.70		0.495	8.04	-52.5	-7.3	±1	±0.2
	Old delta	SH01	SH01		6.54	89.27	33.93	20.67	71.18	123.17	111.31		0.479	8.72	-54.2	-7.4	±1	±0.2
		SH02	SH02		12.84	108.98	126.31	52.02	98.14	298.01	396.12		1.095	7.55	-51.0	-6.9	±1	±0.2
Seawater	Sea	Bohai	SW01		346.43	9025.9	338.80	1077.72	16977.15	2578.3	140.77	58.73	30.485	7.91	-8.4	-3.4	±1	±0.2
Rain	Rain	Rain	R1												-36.2	-6.7	±1	±0.2
Brine	Evaporation	P18	P18		7530	73447	184	28197	174567	35794	634	558	320.353	6.68	-19.3	-0.6	±1	±0.2

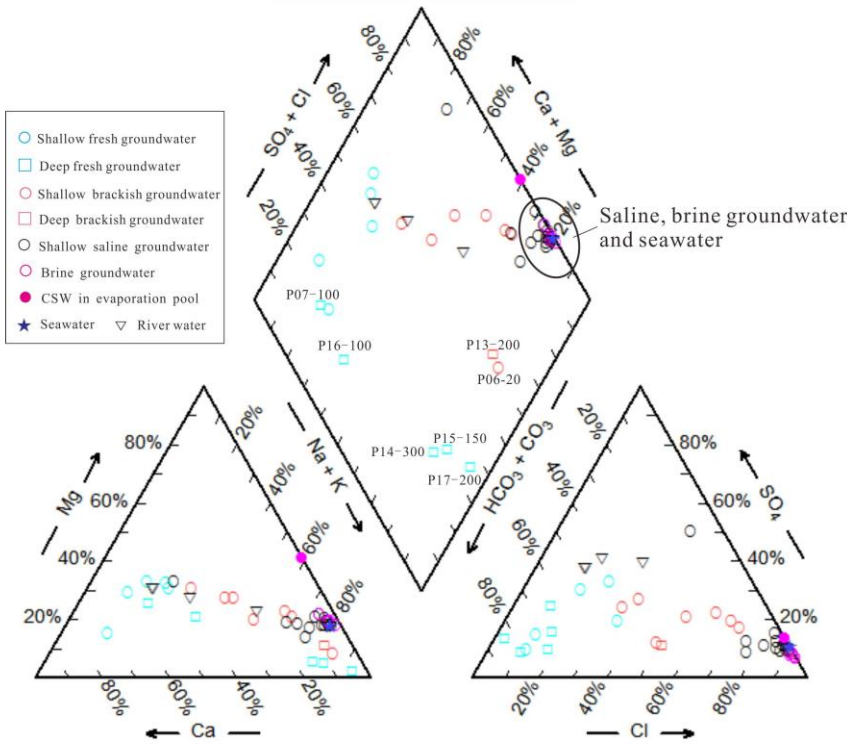

Fig. 3 Piper diagram of the various water samples.

4.2 ^{2}H, ^{18}O stable isotopes

Fig. 4 shows the relationship between deuterium and oxygen-18. The global meteoric water line (GMWL, $\delta^2H=8\cdot\delta^{18}O+10$) is cited from Craig (1961), while the local meteoric water line (LMWL, $\delta^2H=6.6\cdot\delta^{18}O+0.3$) is based on δ^2H and $\delta^{18}O$ isotope data (1985-2003, mean monthly rainfall values) from the Tianjin station, about 100 km southwest of the study area (IAEA/WMO, 2006). The deep groundwater samples ~~mainly plot in the bottom left of the relationship diagram (Fig. 4), which~~ exhibit depleted values of stable isotopes, with values of δ^2H ranging from -75.52‰ to -57.06‰ and $\delta^{18}O$ from -9.82‰ to -7.61‰. Shallow groundwater samples have higher hydrogen and oxygen isotope levels, ranging from -64.6 to -22.46% for δ^2H and -8.74 to -2.07% for $\delta^{18}O$. While the relatively small overall value of fresh and brackish groundwater samples are similar to those of the river samples~~, saline and brine groundwater samples showed a much wider variety (Fig. 4)~~. The ~~shallow groundwater samples, especially~~ saline and brine groundwater, were generally plotted below the LMWL or GMWL, which mean that the water was subjected to evaporation prior to recharge into groundwater (Gibson et al., 1993), or that multiple end-members mixing processes were involved (Han et al., 2011).

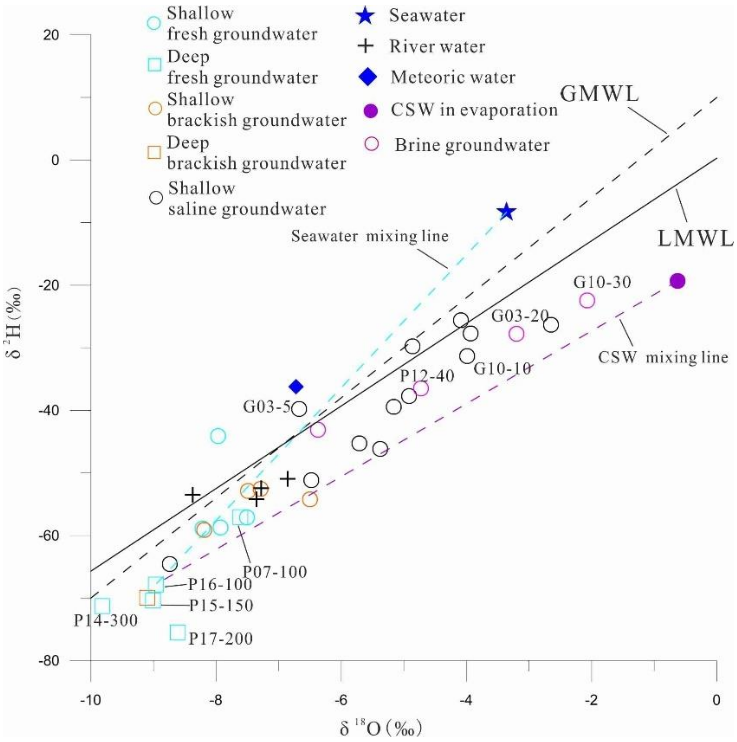

Fig. 4 Stable isotope compositions of different water samples. Seawater mixing line: mixing between deep fresh groundwater and seawater; CSW mixing line: mixing between deep fresh groundwater and CSW.

4.3 Groundwater residence times

The measured ^{14}C activities of groundwater samples range from 0.774 to 105.9 pMC (Table S2). The properties of ^{14}C and sampling depth is shown in Fig. 5, which elucidates the negative correlations , showing that variations of ^{14}C activities could be attributed to radioactive decay aquifer. There are multiple processes that can impact the ^{14}C properties including groundwater mixing and dispersion, long-term variation of atmospheric ^{14}C and free ^{14}C dilution (e.g. carbonate dissolution) (Cartwright et al., 2020). Due to the relative impact of these processes (which are not well established in the study area), the uncertainty regarding the correction of radiocarbon ages to real groundwater ages is very high. Consequently, we estimate groundwater age as a range of the residence time. Uncorrected ages are considered the maximum age, while corrected ages are the minimum age that are determined based on two hypothetical models on carbonate dissolution that mainly affect the ^{14}C contents of water samples (Lee et al., 2016).

Fig.5 shows activities of the ^{14}C in the shallow groundwater are within 30.6 to105.9 pMC. These values indicate relatively modern recharge before atmospheric nuclear testing period of the 1950s and 1960s. The radiocarbon activities in the deep fresh groundwater are less than 12 pMC, which is consistent with the palaeo-water recharge. This indicates that there are weak connection between shallow and deep aquifers. Therefore, we assume that the shallow aquifer is an open system, while the deep aquifer is a closed system. The $\delta^{13}C$ mixing and chemical mass balance (CMB) models are used to estimate to corrective factor q, respectively (Clark and Fritz, 1997).

For $\delta^{13}C$ mixing model, $q = (\delta^{13}C_{DIC} - \delta^{13}C_{CARB}) / (\delta^{13}C_{RECH} - \delta^{13}C_{CARB})$ (Pearson and Hanshaw, 1970), where $\delta^{13}C_{DIC}$ is the measured $\delta^{13}C$ of DIC in groundwater; $\delta^{13}C_{CARB}$ is the $\delta^{13}C$ of DIC from dissolved soil mineral, using $\delta^{13}C_{CARB}$ = 1.5 ‰ (Chen et al., 2003); $\delta^{13}C_{RECH}$ is the $\delta^{13}C$ in water when it reaches the saturation zone. In this study, we use a $\delta^{13}C_{RECH}$ of -15 ‰, which has been suggested as appropriate for soils in northern China dominated by C_4 plants (Currell et al., 2010). The model yielded some relatively low q values (0.59 of G06-15 and 0.65 of G08-15), possibly since several unaccounted factors would contribute to variable $\delta^{13}C_{RECH}$ values, e.g. local methanogenesis and pH or temperatures in the soil zones.

~~given the greater component of C_4 vegetation (such as corn) in the study area, we considered to use $\delta^{13}C_{RECH}$ of -15 ‰ was used for producing a more realistic set of q values.~~

For CMB, $q = mDIC_{rech}/mDIC_{final}$, where $mDIC_{rech}$ is the DIC molar concentration in the recharging water and $mDIC_{final}$ is the DIC molar concentration in the final groundwater. $mDIC_{final}$ was calculated using: $mDIC_{final} = mDIC_{rech} + [mCa + Mg - SO_4 + 0.5(Na + K - Cl)]$ (Fontes and Garnier, 1979). $mDIC_{rech}$ was estimated based on groundwater pH and temperature in the assumed recharge area, e.g., $mDIC_{rech}$ = 10 mmol/L for pH = 6 and T = 15°C (Han et al., 2011).

~~To estimate the corrective factor q, two models were used to account for the dissolution of ^{14}C-free carbon from dissolved inorganic carbon (DIC) in the aquifer.~~

~~Since Fig.5 shows the deep groundwater samples (P16-100, P15-150, and P14-300) contain awere pumped from a confined aquifer,~~

~~which is a relatively closed system, the corrected radiocarbon age was determined using the chemical mass balance model (CMB) (Clark and Fritz, 1997).~~

~~Shallow groundwater samples were collected from semi-confined or phreatic~~

~~aquifers, which are semi-open/open system, and thus~~

The corrected radiocarbon ages are shown in Table S2. ~~and t~~The residence time of deep groundwater ranged from 15959-39050 a B.P., which is significantly longer than that of groundwater in the shallow aquifer (~~about~~ 9510 a B.P. to modern). Moreover, the ages of most brackish and fresh groundwater are modern, while brine has a longer residence period (~~about 1.2-4.3 cal ka~~5590-1245 a B.P.) and a broader variety of saline groundwater samples.

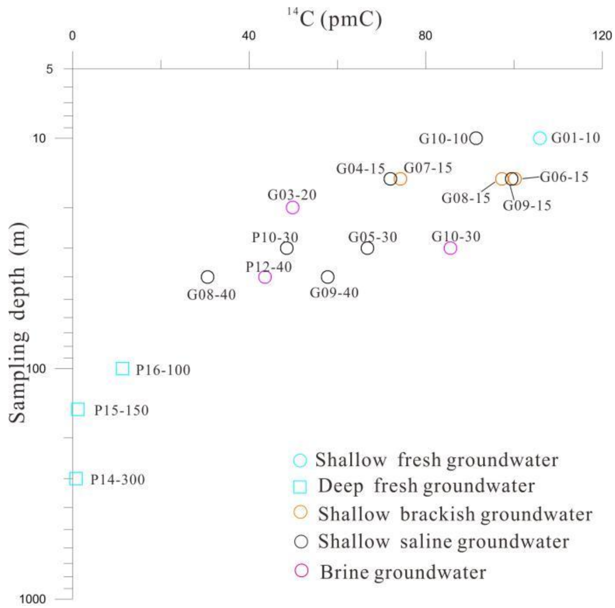

Fig. 5 ^{14}C activity with sampling depth in groundwater.

Table S2 ^{14}C measured value and corrected ages of groundwater samples in the Luanhe River Delta.

Site	Label	^{14}C(pmC)	Uncorrected Radiocarbon Age(a B.P.)	δ ^{13}C (‰, VPDB)	Corrected model	q	Corrected Age(~~cal~~ a B.P.)
G01	G01-10	105.9±0.40	Modern	-12.6	δ^{13}C model	0.85	Modern
G03	G03-20	49.9±0.2	5590	-12.6		0.85	4323
G04	G04-15	72±0.3	2640	-14.7		0.982	2495
G05	G05-30	66.8±0.2	3240	-11.8		0.81	1512
G06	G06-15	100.2±0.4	Modern	-8.2		0.59	Modern
G07	G07-15	74.3±0.3	2390	-10.2		0.71	Modern
G08	G08-15	97.30±0.4	220	-9.2		0.65	Modern
	G08-40	30.6±0.1	9510	-10.4		0.72	6884

G09	G09-15	99.5±0.4	40	-11.5		0.79	Modern
G09	G09-40	57.8±0.2	4410	-11.3		0.78	2367
G10	G10-10	91.4±0.3	720	-14.3		0.96	376
	G10-30	85.6±0.3	1250	-15		1	1245
P14	P14-300	0.774±0.08	39050			0.83	37486
P15	P15-150	1.21±0.09	35460		CMB model	0.83	33951
P16	P16-100	11.33±0.1	17490			0.82	15959

5 Discussion

5.1 Isotopic analysis for origin and recharge of groundwater

Deuterium and oxygen-18 are good tracers for groundwater origin and climatic conditions during recharge periods (Clark and Fritz, 1997). When combined with groundwater residence time, they could further identify modern and palaeo recharge (Han et al., 2014).

The depletion of ^{18}O and ^{2}H values in the deep fresh groundwater (Fig. 4) can be attributed to a cold climate (Kreuzer et al., 2009) and ~~corrected radiocarbon ages~~ residence time of P15-150 and P14-300 samples (range from 33951 ~~and 37486 cal~~ to 39050 a B.P.~~, respectively~~) which may suggest that there was a recharge during the last glacial maximum. ~~Although P16-100 (15959 cal a B.P.) has a slightly higher stable isotope content than deeper groundwater, which is typical of the recharge source as the atmosphere has changed since the last deglaciation~~ The stable isotopes of P16-100 are more enriched, reflecting recharge history of warm climate during the last deglaciation (Hendry and Wassenaar, 2000). The stable isotope values of river samples are similar to those of the shallow brackish and fresh groundwater compositions of the approximate modern age, indicating lateral recharge of surface water locally. Meanwhile, in Fig. 4, G03-5 is close to the rainfall sample, indicating that modern precipitation is a new recharge source. ~~The relatively enriched stable isotopic values and radiocarbon data wide range of residence time (6883 cal B.P. to modern) suggest that the brine and saline groundwater formed during warm Holocene, and they were later recharged by surface water (e.g., G09-15 sample with modern age is closed to the river samples in Fig. 4).~~ T

The trend toward $\delta\ ^{2}H$ and $\delta^{18}O$ enrichment in brine and saline groundwater could be attribute to infiltration of seawater during Holocene transgression period, which has been confirmed by other study in Bohai Sea coast (Li et al., 2017, Du et al., 2016). Additionally, due to mixing of meteoric water, and the subsequent non-equilibrium fractionation of hydrogen isotope during evaporation (Clark and Fritz, 1997), the CSW sample is characterized by ^{18}O enrichment compared to seawater but ^{2}H depletion.

~~The marine and lagoon facies indicate that the study region was inundated by seawater or lagoon water during Holocene sea-level rise, as shown in Fig. 2. The seawater or lagoon water with enriched stable isotopes would recharge the isotopically depleted fresh groundwater, explaining that the $\delta\ ^{18}O$ value of some saline and brine groundwater samples trend toward seawater or CSW in Fig. 4. The significantly high TDS saline groundwater samples, and some brine samples with reduced stable isotope, fall between the seawater and CWS mixing lines, posing several end-member mixing processes as to groundwater salinization, which are further discussed in section 5.3.~~

5.2 Hydrochemical analysis for sources of salinity

~~As previously stated, during Holocene transgression, seawater will infiltrate into aquifers(Santucci et al., 2016), causing groundwater salinity to be significantly affected in the study region . Fig. 6 shows the ion concentrations of various water samples plotted on a Schoeller diagram. The properties of most saline groundwater and brine samples are clearly similar to those of seawater, though some samples have higher concentrations of than that of seawater, implying that the salinity in these groundwater samples is most likely derived from a marine source.~~

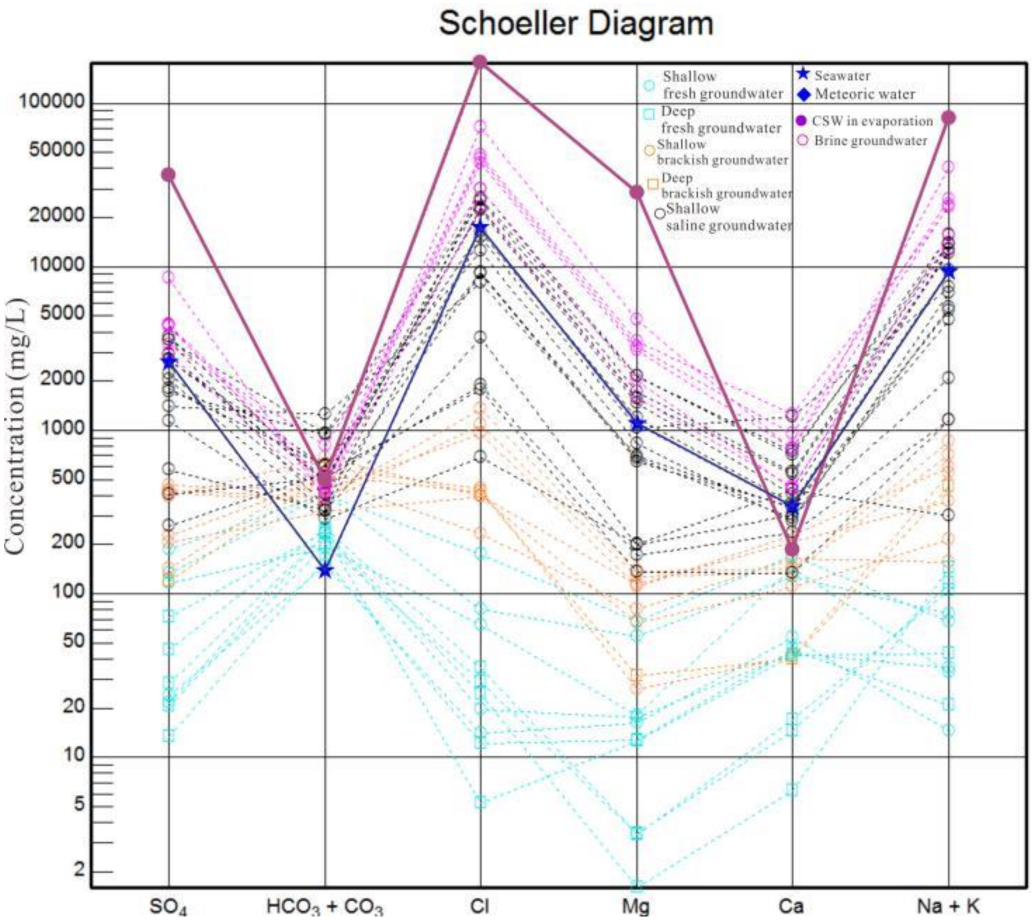

~~Fig. 6 Schoeller diagram of various water samples.~~

For distinguishing the sources of groundwater salinity, the PHREEQC code (Parkurst and Appelo, 2013) was used to measure and plot the theoretical seawater-freshwater mixing line ("mixing line") and seawater evaporation line ("evaporation line") using hydrogeochemical modeling. Using both simulation effects as references to groundwater hydrochemical characteristics (Figs. ~~7~~ 6and ~~8~~7)~~, which could help to distinguish the sources of groundwater salinity~~. For the Na-Cl (Fig. ~~7~~6a), Mg-Cl (Fig. ~~7~~6b), and Br-Cl (Fig. ~~8~~7a) diagrams, whose measured brackish, saline and brine groundwater samples fit quite well to modeling mixing lines and evaporation lines follow linear trends from the least to the most saline. This would strongly demonstrate that, ~~the salinity of salinization groundwater mainly originates from seawater or, the~~

~~CSW which is subject to evaporated seawater~~ the salt in these water samples is mainly marine origin. The major ions concentration in some samples (such as brine) are higher than those in the seawater, suggesting the enriched ions are associated with evaporation processes, rather than seawater intrusion (Colombani et al, 2017).

~~In contrast,~~ Moreover, the samples deviate from the modeling lines (Fig. ~~7~~6c and ~~7~~6d), indicating that there may be other hydrogeochemical processes responsible for the modified ionic compositions: (1) ~~Due to reach saturation, there were loss of ions follow mineral precipitation such as calcite ($CaCO_3$), gypsum ($CaSO_4$), and halite (NaCl) during CWS formation, which consequently explains the decline of Ca^{2+} in P18 and P12 samples in Fig. 76d and, uplift of Br/Cl ratios in brine samples in Fig. 87b.~~ Ca^{2+} depletion of P18 and P12 samples are shown in Fig. 6d. This phenomenon is likely explained by gypsum ($CaSO_4$) precipitation. The evaporation line reveals that the Ca^{2+} composition of evaporating seawater follows a hooked trajectory (Fig. 6d). During evaporation to the point of gypsum saturation, residual CSW becomes progressively decreased Ca^{2+} concentration.. (2) ~~Calcite and gypsum will be dissolved along with surface water during lateral recharge, resulting in brackish groundwater samples plotted above the mixing line, highlighting surface water flushing processes in the study region.~~ Ca^{2+} and SO_4^{2-} excess in most fresh and brackish samples (Fig. 6c and d) could be attributed to mineral dissolution along with stream water recharging, highlighting some degree of dilution with continental runoff since Holocene regression. (3) Decomposition of organic matters which are abundant in marine or lagoon facies sediments can result in release of bromide ions, and thus making the Br/Cl ratios of saline groundwater samples higher than the mixing line (Fig. ~~8~~7b).

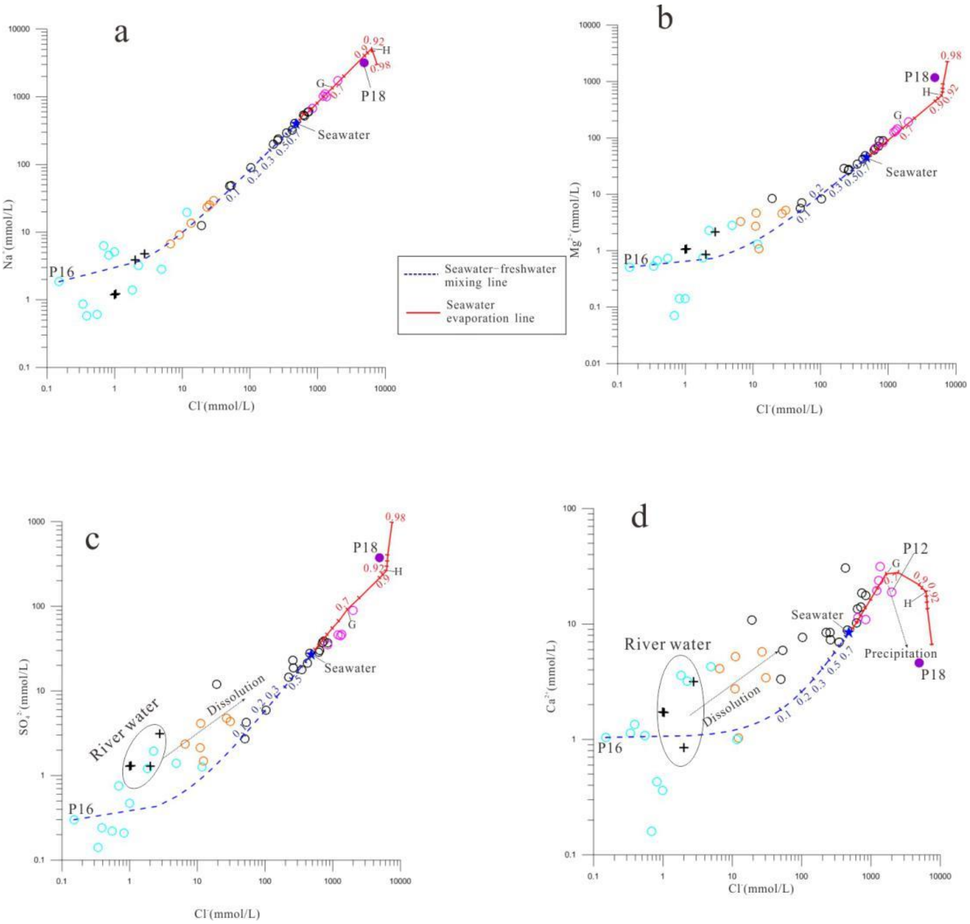

Fig. ~~7~~ 6 Hydrochemical relationship between Cl and major ions of measured samples and simulated results (seawater-freshwater mixing line: theoretical mixing between seawater and deep fresh groundwater, and the blue numbers are mixing ratios of seawater; seawater evaporation line: theoretical evaporation of Bohai seawater, and the red numbers are different evaporation rates) in groundwater. G and H stand for point of precipitation of gypsum, halite respectively. The symbols of samples are same as Fig. 6.

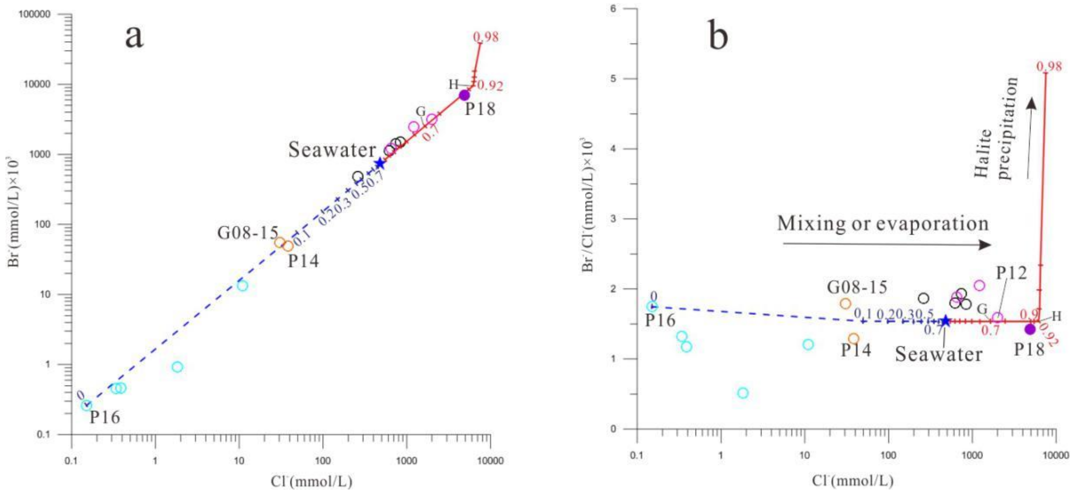

Fig. ~~8~~ 7 Relationship between chloride and bromide content in water samples. Symbols are same as Fig. 7.

5.3 Mixing processes

~~The Concentration of Cl^- and $\delta^{18}O$ were widely used to examine the mixing processes among different end-members in groundwater (Douglas et al., 2000; de Montety et al., 2008; Liu et al., 2017; Han and Currell, 2018).~~

Fig. ~~9~~8depicts the relationship between $\delta^{18}O$ and Cl^- in different water samples. In brine samples, there is ~~a~~ higher Cl^- concentration and lower $\delta^{18}O$ values than in seawater, meaning that simple two end-members mixing cannot adequately explain groundwater salinization. Stable isotopes of high TDS saline and brine samples fall between the seawater and CWS mixing lines, further suggesting potential three end-member mixing processes (Douglas et al., 2000). Therefore, we considered ~~As a result, the~~ SW01 (seawater but with most enriched δ18O) and P18 (most saline but with relatively depleted δ18O) ~~were chosen to represent~~ as two saline end-members.~~, while t~~The P16-100, which is most likely recharged during the Last Deglaciation, was chosen to represent fresh end-members that could have been impacted by ~~infiltration of~~ overlying seawater or CSW during Holocene transgression event. ~~sea-level rise, based on the hypothesis of three end-member mixing processes.~~ In Fig. ~~9~~8, an inferred salinization zone was established that included almost all saline and brine groundwater samples, demonstrating the salinization processes in which fresh groundwater mixed with either seawater, CSW, or a mixture of both.

The fresh and brackish groundwater samples, on the other hand, have low Cl^- concentrations and depleted ^{18}O, deviating from the assumed salinization zone but approaching the river samples in Fig. ~~8~~7, implying a river water-groundwater mixing trend. The LH02 (depleted $\delta^{18}O$) and SH02 (relatively enriched $\delta^{18}O$) were selected to represent river water end-members range for different continental runoff in study area, while the G09-15 (saline but with river-like stable isotope) was considered as a groundwater end-member. There is a presumed freshening zone could form between two river water-groundwater mixing lines, indicating occurrence of freshening processes which would be in agreement with continental runoff dilution discussed in section 5.2.

~~This trend will wash out the above-mentioned salinization, owing to lateral recharge of surface water towards the continental area, which led to a decrease in salinity in groundwater over time, as shown in the G09-15 sample. In addition, a presumed freshening zone could form between two river water-groundwater mixing lines, indicating freshening processes in the Luanhe River Delta that may have been retained since the delta progradation.~~

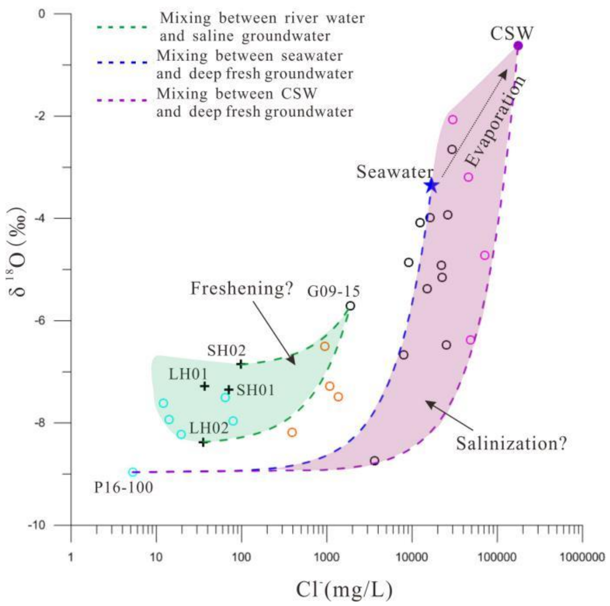

Fig. ~~9~~ 8 Relationship between Cl and $\delta^{18}O$ of different water samples as means to various mixing processes in the Luanhe River Delta. The symbols are same as Fig. 6. The green area is assumed freshening zone, and the purple area is assumed salinization zone.

6 Interpretation of palaeo-environmental development

~~Previously, we introduced that the continental area of the Luanhe River Delta is mainly affected by MIS5 and Holocene marine transgression (see 2.3). Assuming that the MIS5 marine transgression event resulted in palaeo-seawater intrusion in the study region. Overlying MIS 5 marine deposits, the evidence of channel deposits in core BXZK02 (dated between 100 ka B.P. and 10 ka B.P., He et al., 2020) and lacustrine deposits in core FG01 (Xu et al, 2011) both imply that fresh surface water flushing the upper saline aquifer would have taken a long time after MIS 5 marine transgression. In addition,~~ Based on analysis of a range of evidence related to Quaternary geographic evolution, it is possible to understand the change of hydrogeological conditions in the past (Van Engelen et al., 2018). The Pleistocene transgression events-related to Marine isotope stage (MIS) 3 and 5-have been observed to once reach the study area by other authors (Wang et al., 1981; Peng et al., 1981; Li et al., 1982; Xu et al., 2018), which would be resulted in groundwater salinization. Since the last deglaciation (about 15 ka B.P.), the palaeo-coast ~~zone~~ line has approximately 100 m depth below present sea level along the shelf edge (Liu et al., 2020; Li et al., 2014). Stronger river down-cutting and flushing in the study region would have been helped a large fresh recharge of groundwater. ~~hydraulic gradient and a large shift in palaeoclimate (Xu et al., 2011), resulting in the fresh groundwater found near the core BXZK02 as~~ For example, P16-100 (fresh water) was sampled from a relatively deep position (100 m below surface) has an estimated groundwater age between 15959 to 17490 ~~with a corrected radiocarbon age of 15959 cal~~ a B.P., which is likely to provide evidence that the salinization groundwater related to MIS 5 and/or 3 marine transgression could have been flushed out until the Latest Pleistocene. Accordingly, we believe that the observed saline groundwater in the Luanhe River Delta is probably related to the subsequent Holocene marine transgression. This research develops the evolutionary pattern of saline groundwater, as shown in Table 1 and Fig. ~~10~~9, ~~based on hydrochemical and isotopic analysis, together with the sedimentary evolution of the study region after the Holocene. T~~three phases are synthesized and reconstructed, as follows.

Table ~~3~~1 Saline groundwater evolution processes in study area

Evolution stage	Groundwater evolution processes		Influencing factors			Major hydrogeochemical processes	Sediments
	Evolutionary pattern	Factors	Palaeoclimate	Geological setting	Others		
Phase 3 The development of new delta (3. 5ka B. P. to present)	Freshening	Wash-out of surface water	temperate, slightly semi-humid	Development of surface straem	irrigation return	Mixing and leaching	Holocene alluvial deposit or artificial fill Bottom sediments age about 1795—302 a B. P. (Xu et al., 2020 He et al., 2020)
	Deceleration of brine formation	Limitations of seawater evaporation		Diversion of channels and lagoon filled by diluvial deposit	artificial reclamation and offshore levees		Holocene lagoon facies Bottom sediments age about 5995—1600 a B. P. (Cheng et al., 2020 He et al., 2020)
Phase 2 The development of old delta (7 to 3. 5ka B. P.)	Brine formation	Sseawater evaporation and CSW infiltrating	temperate, slightly arid	Deceleration of sea-level rising, development of delta, and coastal lagoons have been active	Tides or storm	Mixing, leaching, evaporation, and mineral precipitation	Holocene delta facies Bottom sediments age about 6675—3695 a B. P. (He et al., 2020)
Phase 1 Holocene transgression (12 to 7ka B. P.)	Groundwater salinization	Palaeo-seawater intrusion	temperate-warm, humid	Deglaciation of ice sheet, rapid rising of sea level, Holocene transgression		Mixing	Holocene marine facies Bottom sediments age about 8620—5595 a B. P. (Li et al., 1982) Late Pleistoncene continental facies (Xu et al., 2020 He et al., 2020)

Phase 1: Transgressive system tract-Holocene transgression stage (9-7 ka B.P.)

Global sea level was affected by deglaciation of the ice sheet (Fairbanks, 1989), causing sea level to rise rapidly during the deglaciation period (15.4-7 ka B.P.) (Li et al., 2014).~~ Previous studies have shown that seawater reached the southwestern Bohai Bay at 9.9 ka B.P. (Xu et al., 2015), and the present coastline of the study area at about 9 ka B.P. (Xu et al., 2020), and then the Holocene marine transgression approached its maximum in the Bohai Sea region at about 7 ka B.P. (Xue 2009, 2014). ~~It could be summarized that the Holocene transgression stage, which occurred between 9 and 7 ka B.P, resulted in the study area being inundated by seawater (Xu et al., 2015; Xue 2009, 2014) (Fig. ~~10~~9a). On the one hand, there would have been a tendency for the denser seawater to infiltrate through the aeration zone~~ and to mix with the fresh groundwater under the aquifer ~~(Santucci et al., 2016); on the other hand, sea-level rising would cause the seawater-freshwater interface to move landward (Ferguson and Gleeson, 2012), both of which contributed to palaeo-seawater intrusion. ~~The characteristics of ionic components in the salinized groundwater are similar to those of seawater in Fig. 6. ~~The G08-40 contains TDS of 27.173 g/L, which is more similar to that of SW01.

Simultaneously, the ~~corrected radiocarbon age is~~ residence time (9810-6884 ~~cal~~ a B.P.)~~,~~ indicate trapped palaeo-seawater at low-permeability aquitard sediments still exists and may be another critical salinity source for neighboring aquifers in the coastal zone (Post and Kooi, 2003; Lee et al., 2016).

The presence of palaeo-seawater intrusion during Quaternary has been recorded in other coastal regions worldwide (Groen et al., 2000; Bouchaou et al., 2009, Tran et al., 2012; Han et al., 2020). For the works described above, the salinity of groundwater after salinization could not exceed that of seawater due to palaeo-seawater intrusion.

Other salinization processes that occurred during palaeo-environmental growth are likely to be correlated with such brine groundwater.

Phase 2: Highstand system tract-Old Luanhe River Delta development (7-3.5 ka B.P.)

~~Since about 7 ka B.P. (Saito et al., 1998; Zong, 2004), global marine deltas such as the Nile Delta, Mississippi Delta, Yangtze Delta, and Luanhe River Delta have developed (Stanley and Warne, 1994).~~

The good fit between the measured hydrochemistry and simulated evaporation lines (Fig. 6 and 7) is an indicator that the brine samples were associated with the seawater which was exposed to evaporation during geological history. Previous research has revealed ~~sediments characteristic of a lagoon environment in the western study region, indicating that this~~ that lagoon environment was active during the progradation of the old Luanhe River Delta between 7 and 3.5 ka B.P. (He et al., 2020; Xu et al., 2020). Meanwhile, ~~after around 5500 B.P., the humid palaeoclimate in this region has changed to be slightly arid~~ the relatively arid climate had been developed since 5500 a B.P., which may lead to increased evaporation (Jin, 1984). The ancient lagoon would be an ideal location for evaporating seawater that had been trapped due to storms or tides (Fig. ~~10~~9b). As a result, concentrated saline water (CSW) with salinity higher than seawater would have created, and the CSW ~~kept in the lagoon~~ would go through two processes: (1) infiltrating and descending to the lower part of the aquifer due to its higher density, and combining with the salinized groundwater from phase 1, resulting in a three end-members mixing scenario in the relationship diagram (Fig. ~~9~~8). (2) After reaching saturation during the later stages of evaporation, mineral precipitation, such as gypsum, calcite, and halite, would occur, and this would be subjected to redissolution by meteoric waters or seawater, resulting in high salinity water that would then be subjected to the above process; The Br/Cl ratios in certain fresh or brine groundwater samples deviate from the evaporation line (Fig. ~~8~~7b), which may be related to halite precipitation and redissolution. These two processes caused groundwater salinity to rise even further, resulting in the formation of brine groundwater with 3 times the TDS of seawater, such as G03-20 with a range of resident time of 4323 to 5590 ~~cal~~ a B.P.

Phase 3: New Luanhe River Delta development (3.5 ka B.P. -present)

Since about 3500 a B.P., a nearly 90-degree diversion of the Luanhe River channel in the study area resulted in new delta development (Wang et al., 2007; Xue et al., 2016). There are some signs of a lagoon environment in the new Luanhe River Delta~~, such as core LQZ14 in Fig. 1a, which includes a lagoon deposit with a radiocarbon date of about 2 ka B.P.~~(Cheng et al., 2020), and, as previously discussed, the brine groundwater sample G10-30 would be attributed to evaporation in a lagoon setting (Fig. ~~10~~9c).

However, some factors are likely to limit the CSW formation in the study area: (1) the relatively low evaporation capacity due to semi-humid climate since ~~the palaeoclimate of the study area changed to semi-humid at~~ about 2.5 ka B.P. (Jin, 1984), ~~contributing to low evaporation capacity;~~ (2) the diluvial deposit or artificial reclamation would have filled the coastal low-land such as lagoons, and (3) offshore levees prevent the seawater from flooding inland during storms or tides. These factors may also explain why, unlike the old Luanhe River Delta, the current Luanhe River Delta does not have high TDS brine groundwater.

In addition, the brackish and low TDS saline groundwater with relatively modern age (e.g. G09-15), and river-like stable isotopes (Fig. 4 and 8), are compelling evidence that freshening processes have occurred in the delta plain. Since the semi-humid palaeoclimate, some abandoned channels have developed into small rivers after the diversion of the ancient Luanhe River (Gao, 1981), such as the Suhe River and Shahe River. Firstly, the lateral recharge from the surface stream plays a role in washing out the salty groundwater. Secondly, due to the inefficiency of saline groundwater throughout human history, river irrigation has been commonly used for agricultural activities in the study region, freshening the upper saline aquifer (Fig. ~~10~~9c). ~~The brackish and low TDS saline groundwater with modern age (e.g. G08-15, G09-15), and rapid increase in Electric Conductivity profile (Dang et al., 2020), are compelling evidence that freshening processes have occurred in the delta plain, as shown by the $\delta^{18}O$-Cl^- relationship diagram (Fig. 9).~~ Some groundwater samples found above the seawater mixing line in the Ca-Cl and SO_4-Cl relationship diagrams (Fig. ~~7~~6c, d) may be related to mineral dissolution during river water or irrigation recharge. However, saline groundwater can be washed out over time in coastal zones with low-permeable marine layers and a low hydraulic gradient (van Engelen et al., 2019; Han et al., 2020).

In summary, the evolution of saline groundwater in the study area is a result of palaeo-environment development such as sea-level change, palaeogeography, and palaeoclimate, and is significantly affected by human activities. ~~Sea-level rise led to palaeo-seawater intrusion. After deceleration of sea-level rise, there would be formation of brine groundwater and slow wash-out during the delta development.~~ The coastal brine groundwater is a special product of geological evolution, which have been found in Bohai Sea coast such as Bohai Bay (Li et al., 2017) and Laizhou Bay (Han et al., 2014). The change in sea level over the Late Pleistocene would have favoured marine intrusion and similar sedimentary environment in Bohai coast, allowing this study infers the following conditions for ~~its~~ brine formation: (1) stable evaporative environments (e.g. lagoon), (2) suitable climatic conditions (e.g. arid), (3) seawater entering evaporative environments (e.g. storm or tide), and (4) long-term scale for salinity accumulation.

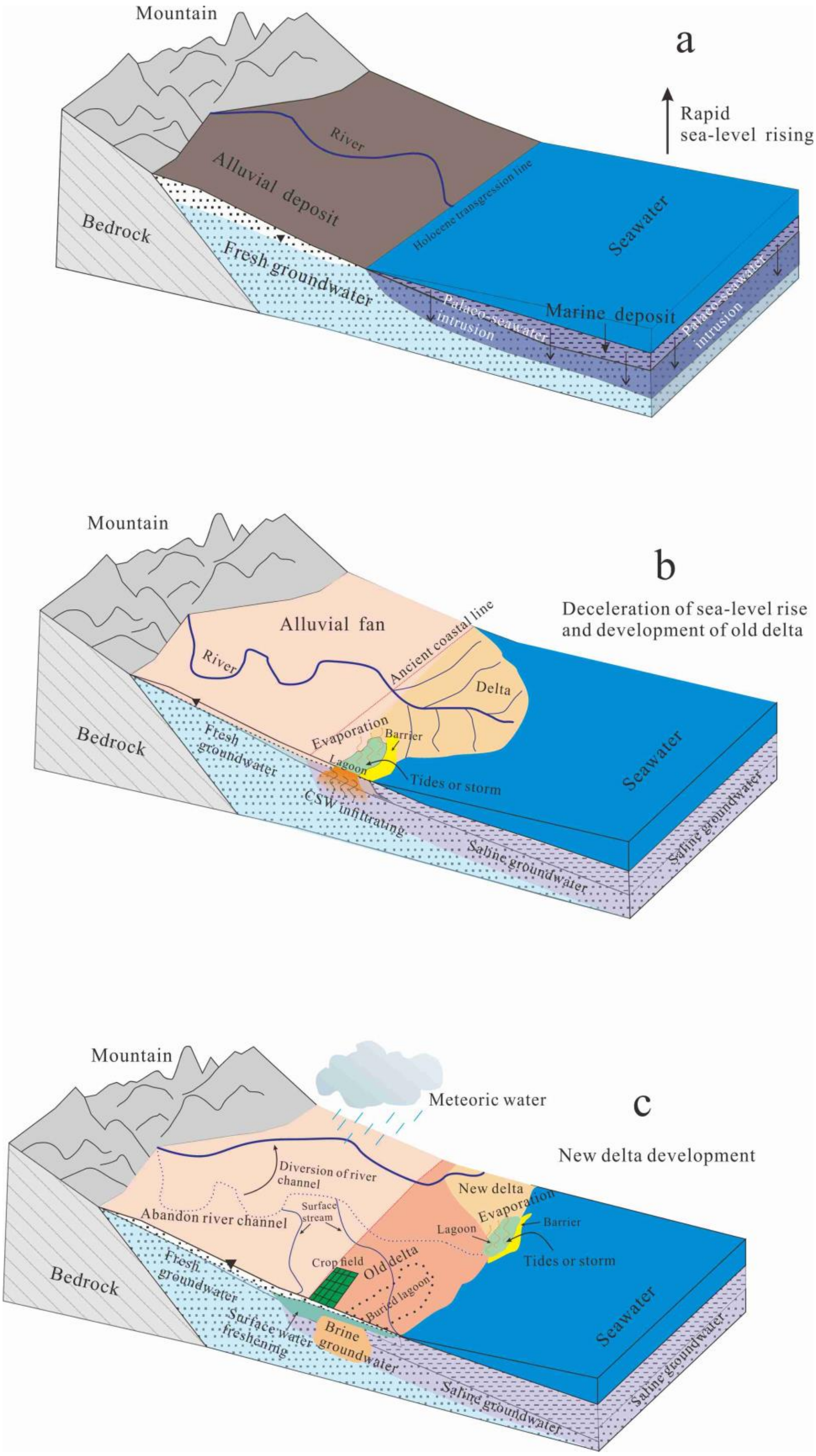

Fig. ~~10~~ 9 Diagram of palaeoenvironmental development since Holocene and evolutionary pattern of saline groundwater.

7 Conclusions

~~The brackish, saline and brine groundwater have been observed at least 20 km inland in the Luanhe River Delta.~~ In this study, we used a range of isotopic-geochemical methods to analyze the recharge and salinity source of groundwater in the Luanhe River Delta. ~~-as well as the salinization and freshening processes, using hydrochemical and isotopic methods~~. The isotopic results (^{2}H, ^{18}O, ^{14}C) show that deep confined groundwater was recharged during the Late Pleistocene cold period, shallow saline and brine groundwater was recharged during the warm Holocene period, and shallow brackish and fresh groundwater was mainly recharged by surface water. The hydrogeochemical modeling (PHREEQC) results showe that seawater or evaporated seawater is the primary salty source in salinized groundwater. The variation in the ^{18}O-Cl relationship of multiple water samples further indicates multiple end-member mixing, which is useful assess the salinization and/or freshening processes in aquifers. ~~The evolution of saline groundwater and its connection to palaeo-environmental settings were studied using sedimentary characteristics as multiple lines of evidence. The following are the key findings:~~ Our study shows that multiple water types are particularly associated with complex geographic evolution in coastal areas. The variation in sea-levels (when it rises) causes lowland coastal areas to be inundated by seawater, which induces palaeo-seawater intrusion. The costal deltas developed after significant drop in the sea levels. The concentration of saline water in the lagoon environment at the delta-front continuously provided salinity to the groundwater. Thus, under the effects of evaporation, mixing, and dissolution, brine groundwater was formed. In contrast, the lateral recharge of surface water and irrigation return would cause slow wash-out of salinized groundwater in the delta plain.

(1) Different groundwater recharges are identified using environmental isotope analysis (^{2}H, ^{18}O, ^{14}C). For the groundwater and Bohai seawater samples, hydrogeochemical modeling (PHREEQC) was used, with a fresh groundwater-seawater mixing line and a Bohai seawater evaporation line as assumptions. The measured and simulated value agrees well, implying that seawater or concentrated saline water is the primary salty source of groundwater salinization. The variation in the ^{18}O-Cl relationship of multiple water samples further indicates that majority of the saline and brine groundwater originates from three mixing end-members: fresh groundwater, seawater, and concentration saline water. However, there would be some freshening processes observed in brackish groundwater samples, suggesting the wash-out of saline groundwater by surface water.

(2) The evolution of saline groundwater could be reconstructed and summarized using the palaeoenvironmental information contained in the sediments. Given the sea level fell to the lowest position during the Last Glaciation, the palaeochannels downcutting would have contributed to the intense recharge of groundwater by river water. This study infers that fresh groundwater at upper aquifers before the Holocene marine transgression reached the study area. The evolution of saline groundwater has been traced to three distinct phases: (1) The study area was gradually submerged by seawater around 9-7 ka B.P., and groundwater salinization occurred due to palaeo-seawater intrusion. (2) During the development of the old Luanhe River Delta between

~~7 and 3.5 ka B.P., the concentration of saline water in the lagoon environment of delta-front continuously provided salinity to the groundwater, and under the effects of evaporation, mixing, and dissolution, some brine groundwater was formed. (3) After the Luanhe River channel's diversion at about 3.5 ka B.P., the new Luanhe River Delta began to develop. On the one hand, the diluvial deposit and human activities limit the formation of brine groundwater; on the other hand, the lateral recharge of surface water and irrigation return would cause partly slow wash-out of saline groundwater in the delta plain.~~

Given that most coastal zones around the world experienced transgression/regression events in the Quaternary period, the findings of this work will promote better understanding of the origin of salinization in coastal aquifers. In addition, it is important to recognize the potential leak of connate saline groundwater previously preserved in adjunct aquifers that can occur due to over-extraction of deep groundwater. ~~In coastal zones which similar to this study area, over-extraction of deep groundwater may not only lead the interface of seawater-freshwater to move landward but also cause groundwater salinization by leakage of saline water in adjunct aquifers.~~ If this leak occurs, it will cause widespread salinization of fresh groundwater, particularly if high-salinity brine is presented~~, which will endanger water quality, like the groundwater salinization in Laizhou Bay~~. To effectively avoid pollution from saline groundwater movement, this study recommends extensive characterization of groundwater interface dynamics, such as fresh/saline, fresh/brine, and brine/seawater interfaces and also maintain continuous monitoring of water quality and levels across the aquifers.~~of~~

~~groundwater quality and levels, as well as successful well policies and programs for groundwater resource use.~~

Authors contribution

Xianzhang Dang: Conceptualization, Formal analysis, Investigation, 3 Writing-Original Draft, Data curation.

Maosheng Gao: Funding acquisition, Methodology, Supervision, Investigation, Writing-Review & Editing.

Zhang Wen: Supervision, Writing-Review & Editing.

Guohua Hou: Project administration, Investigation.

Hamza Jakada: Writing-Review & Editing.

Daniel Ayejoto: Writing-Review & Editing.

Qiming Sun: Investigation.

Acknowledgement

This study was financially supported by the National Natural Science Foundation of China (41977173), National Key Research and Development Program of China (No.2016YFC0402800) and the National Geological Survey Project of China Geology Survey (No. DD20211401). The authors would like to thank Sen Liu, Chenxin Feng, Chen Sheng, Xueyong Huang and Haihai Zhuang, for their help and support in collecting field data and conducting geological survey.

References

Akouvi, A., Dray, M., Violette S.,et al., 2008. The sedimentary coastal basin of Togo: example of a multilayered aquifer still influenced by a palaeo-seawater intrusion. Hydrogeology Journal, 16, 419-436, doi: 10.1007/s10040-007-0246-1.

Aquilina, L., Vergnaud-Ayraud, V., Les Landes, A. A., et al., 2015. Impact of climate changes during the last 5 million years on groundwater in basement aquifers, Scientific Reports, 5, 14132, doi: 10.1038/srep14132.

Bouchaou, L., Michelot, J.L., Qurtobi, M., et al., 2009. Origin and residence time of groundwater in the Tadla basin (Morocco) using multiple isotopic and geochemical tools. Journal of Hydrology, 379, 323-338, doi: 10.1016/j.jhydrol.2009.10.019.

Cary, L. et al., 2015. Origins and processes of groundwater salinization in the urban coastal aquifers of Recife (Pernambuco, Brazil): A multi-isotope approach. Science of the Total Environment, 530-531, 411-429, doi: 10.1016/j.scitotenv.2015.05.015.

Cartwright, I., Currell, M., Cendon, D., Meredith, K., 2020. A review of the use of radiocarbon to estimate groundwater residence times in semi-arid and arid areas. J. Hydrol., 580, 124247. https://doi.org/10.1016/j.jhydrol.2019.124247.

Chen, Z.Y., Qi, J.X., Xu, J.M., Xu, J.M., Ye, H., Nan, Y.J., 2003. Paleoclimatic interpretation of the past 30 ka from isotopic studies of the deep confined aquifer of the North China Plain. Applied Geochemistry, 18, 997-1009, doi: 10.1016/S0883-2927(02)00206-8.

Cheng, L.Y., Xu, Q.M., Guo, H., et al., 2020. The Late Holocene Stratum and evolution in the Luanhe River Delta. Quaternary Sciences, 40(3), 751-763, doi: 10.11928/j.issn.10017410.2020.03.13(In Chinese with English abstract).

Clark, I.D., and Fritz, P., 1997. Environmental Isotopes in Hydrogeology. Lewis Publishers, New York.

Colombani, N., Cuoco, E., Mastrocicco, M., 2017. Origin and pattern of salinization in the Holocene aquifer of the southern Po Delta (NE Italy). Journal of Geochemical Exploration, 175(2017): 130-137, doi: 10.1016/j.gexplo.2017.01.011.

Cost Environment Action 621, 2005. Groundwater management of karstic coastal aquifers. European Communities, Luxembourg.

Costall A. R., Harris B. D., Teo B., Schaa R., Wagner F.M., Pigois J. P., 2020. Groundwater Throughflow and Seawater intrusion in High Quality coastal Aquifers. Scientific Reports, 10: 9866, doi: 10.1038/s41598-020-66516-6.

Craig, H., 1961. Standard for reporting concentration of deuterium and oxygen-18 in natural water. Science, 133, 1833-1834, doi: 10.1126/science.133.3467.1833.

Currell, M.J., Cartwright, I., Bradley, D.C., Han, D.M., 2010. Recharge history and controls on groundwater quality in the Yuncheng Basin, north China. Journal of Hydrology, 385, 216-229., doi: 10.1016/j.jhydrol.2010.02.022.

Dang, X.Z., Gao, M.S., Wen, Z., Jakada, H., Hou, G.H., Liu, S., 2020. Evolutionary process of saline groundwater influenced by palaeo-seawater trapped in coastal deltas: A case study in Luanhe River Delta, China. Estuarine, Coastal and Shelf Science, 244, 106894, doi: 10.1016/j.ecss.2020.106894.

de Montety, V., Radakovitch, O., Vallet-Coulomb, C., et. al., 2008. Origin of groundwater salinity and hydrogeochemical processes in a confined coastal aquifer: case of the Rhone delta (Southern France). Applied Geochemistry, 23(8), 2337-2349, doi: 10.1016/j.apgeochem.2008.03.011.

Delsman, J. R., Huang, K. R. M., Vos, P. C., de Louw, P. G. B., Oude Essink, G. H. P., Stuyfzand, P. J., and Bierkens, M. F. P., 2014. Paleo-modeling of coastal saltwater intrusion during the Holocene: an application to the Netherlands. Hydrology and Earth System Sciences, 18(10), 3891-3905, doi: 10.5194/hess-18-3891-2014.

Douglas, M., Clark, I.D., Raven, K., et al., 2000. Groundwater mixing dynamics at a Canadian Shield mine. Journal of Hydrology, 235, 88-103, doi: 10.1016/S0022-1694(00)00265-1.

Du, Y., Ma, T., Chen, L., et a., 2015. Genesis of salinized groundwater in Quaternary aquifer system of coastal plain, Laizhou Bay, China: Geochemical evidences, especially from bromine stable isotope. Applied Geochemistry, 2015, 59:155-165, doi: 10.1016/j.apgeochem.2015.04.017.

Du, Y., Ma, T., Chen L., et al., 2016. Chlorine isotopic constraint on contrastive genesis of representative coastal and inland shallow brine in China, Journal of Geochemical Exploration, 170 (2016): 21-29, doi: 10.1016/j.gexplo.2016.07.024.

Edmunds, W. M., 2001. Palaeowaters in European coastal aquifers-the goals and main conclusions of the PALAEAUX project, Geological Society London Special Publications, 189, 1-16, doi: 10.1144/GSL.SP.2001.189.01.02.

Fairbanks, R.G., 1989. A 17,000-year glacio-eustatic sea level record: influence of glacial melting rates on the Younger Dryas event and deep ocean circulation. Nature, 342, 637-647, doi: 10.1038/342637a0.

Feng, J. and Zhang, W., 1998. The evolution of the modern Luanhe River delta, north China. Geomorphology, 25 (3), 269-278, doi: 10.1016/S0169-555X(98)00066-X.

Ferguson, G. and Gleeson, T., 2012. Vulnerability of coastal aquifers to groundwater use and climate change. Nature Climate Change, 2, 342-345, doi: 10.1038/nclimate1413.

Fontes, J.C. and Matray, J.M., 1993. Geochemistry and origin of formation brines from the Paris Basin, France. 1. Brines associated with Triassic salts. Chemical Geology, 109, 149-175, doi: 10.1016/0009-2541(93)90068-T.

Gao, S.M., 1981. Facies and sedimentary model of the Luan River delta. Acta Geographica Sinica, 48 (3), 303-314, doi: 10.11821/xb198103006 (in Chinese with English abstract).

Geriesh, M. H., Balke, K.-D., El-Rayes, A. E., and Mansour, B. M., 2015. Implications of climate change on the groundwater flow regime and geochemistry of the Nile Delta, Egypt, Journal of Coastal Conservation, 19, 589-608, doi: 10.1007/s11852-015-0409-5.

Giambastiani B.M.S., Colombani N., Mastrocicco M., Fidelibus M.D., 2013. Characterization of the lowland coastal aquifer of Comacchio (Ferrara, Italy): Hydrology, hydrochemistry and evolution of the system. Journal of Hydrology, 501: 35-44, doi: 10.1016/j.jhydrol.2013.07.037.

Gibson, J.J., Edwards, T.W., Bursey, G.G., Prowse, T.D., 1993. Estimating evaporation using stable isotopes: quantitative results and sensitivity analysis for two catchments in Northern Canada. Nordic Hydrology. 24, 79-94, doi: 10.2166/nh.1993.0015.

Groen, J., Velstra, J., Meesters, A., 2000. Salinization processes in paleowaters in coastal sediments of Suriname: evidence from δ^{37}Cl analysis and diffusion modelling. Journal of Hydrology, 234, 1-20, doi: 10.1016/S0022-1694 (00)00235-3.

Han, D.M., Kohfahl, C., Song, X.F., et al., 2011. Geochemical and isotopic evidence for Palaeo-Seawater intrusion into the south coast aquifer of Laizhou Bay, China. Applied Geochemistry 26 (5), 863-883, doi: 10.1016/j.apgeochem.2011.02.007.

Han, D. M., Song, X. F., Currell, M. J., et al., 2014. Chemical and isotopic constraints on the evolution of groundwater salinization in the coastal plain aquifer of Laizhou Bay,China, Journal of Hydrology, 508, 12–27, doi: /10.1016/j.jhydrol. 2013.10.040.

Han, D.M., Currell, M.J., 2018. Delineating multiple salinization processes in a coastal plain aquifer, northern China: hydrochemical and isotopic evidence. Hydrology and Earth System Science, 22, 3473-3491, doi: 10.5194/hess-22-3473-2018.

Han, D.M., Cao G.L., Currell, M.J., et al., 2020. Groundwater salinization and flushing during glacial-interglacial cycles: insights from aquitard porewater tracer profiles in the North China Plain, China. Water Resource Research, 56 (11), doi: 10.1029/2020WR027879.

He L., Amorosi A., Ye S.Y., et al., 2020. River avulsions and sedimentary evolution of the Luanhe fan-delta system (North China) since the late Pleistocene. Marine Geology, 425,106194, doi: 10.1016/j.margeo.2020.106194.

Hendry, M.J. and Wassenaar, L.I., 2000. Controls on the distribution of major ions in pore waters of thick surficial aquitard. Water Resources Research, 36 (2), 503-513, doi: 10.1029/1999WR900310.

IAEA/WMO, 2006. Global Network of Isotopes in Precipitation, The GNIP Database, Vienna, available at: http://www-naweb.iaea.org/napc/ih/IHS_resources_gnip. html.

Jiao, J.J. and Post, V., 2019. Coastal Hydrology. Cambridge University Press, New York.

Jin, X.F., 1984. The spore-pollen assemblages and the stratigraphy and palaeogeography in western Bohai Sea since late Pleistocene . Marine Science Bullition 3, 16-24, doi: CNKI:SUN:HYKX.0.1984-03-003 (in Chinese with English abstract).

Kooi, H., Groen, J., and Leijnse, A., 2000. Modes of seawater intrusion during transgressions, Water Resource Research, 36, 3581–3589, doi: 10.1029/2000wr900243.

Kreuzer, A.M., Rohden, C.V., Friedrich, R., et al., 2009. A record of temperature and monsoon intensity over the past 40 kyr from groundwater in the North China Plain. Chemical Geology, 259, 168-180, doi: 10.1016/j.chemgeo.2008.11.001.

Larsen, F., Tran, L. V., Van Hoang, H., et. al., 2017. Groundwater salinity influenced by Holocene seawater trapped in incised valleys in the Red River delta. Nature Geoscience, 10, 376-381, doi: 10.1038/ngeo2938.

Lee, S., Currell, M., and Cendon, D. I., 2016. Marine water from mid-Holocene sea level highstand trapped in a coastal aquifer: Evidence from groundwater isotopes, and environmental significance. Science of the Total Environment, 544, 995-1007, doi: 10.1016/j.scitotenv.2015.12.014.

Li, G.X., Li, P., Liu, Y., et al., 2014 Sedimentary system response to the global sea level change in the East China Seas since the last glacial maximum. Earth-Science Reviews, 139 (2014), 390-405, doi: 10.1016/j.earscirev.2014.09.007.

Li, H.M. and Wang, J.D., 1983. Palaeomagnetic study on drill core from northern Bohai coastal plain. Geochimica, 2, 196-204 (in Chinese with English abstract).

Li, J., Liang, X., Jin, M. G., et. al., 2013. Geochemical signature of aquitard pore water and its paleo-environment implications in Caofeidian Harbor, China. Geochemical Journal, 47, 37-50, doi: 10.2343/geochemj.2.0238.

Li, Y.F., Gao, S.M. and An, F.T., 1982. A preliminary study of the Quaternary marine strata and its paleogeographic significance in the Luanhe delta region. Oceanologia et Limnologia Sinica, 13 (5), 433-439, doi: CNKI:SUN:HYFZ.0.1982-05-005 (in Chinese with English abstract).

Liu, S., Tang, Z., Gao, M. et. al., 2017. Evolutionary process of saline-water intrusion in Holocene and Late Pleistocene groundwater in southern Laizhou Bay. Science of the Total Environment, 607-608, 586-599, doi: 10.1016/j.scitotenv.2017.06.262.

Liu, J., Wang, H., Wang, F., et al., 2016. Sedimentary evolution during the last ~ 1.9 Ma near the western margin of the modern Bohai Sea. Palaeogeogrphy, Palaeoclimatology, Palaeoecology, 451, 84-96, doi: 10.1016/j.palaeo.2016.03. 012.

Ma, F. S., Wei, A. H., Deng, Q. H., et. al., 2014. Hydrochemical Characteristics and the Suitability of Groundwater in the Coastal Region of Tangshan, China. Journal of Earth Science, 26 (6), 1067-1075, doi: 10.1007/s12583-014-0492-9.

Martínez, M.L., Intralawan, A., Vázquez, G., et. al., 2007. The coasts of our world: Ecological, economic and social importance. Ecological Economics, 63 (2-3), 254-272, doi: 10.1016/j.ecolecon.2006.10.022.

Niu, Z.X., Jiang X.W. and Hu, Y.Z., 2019. Characteristics and causes of hydrochemical evolution of deep groundwater in the Luanhe delta. Hydrogeology and Engineering Geology, 46 (01), 27-34, doi: 10. 16030/j. cnki. issn. 1000-3665. 2019. 01.04 (in Chinese with English abstract).

Parkhurst, D.L., Appelo, C.A.J., 2013: Description of input and examples for PHREEQC version 3-a computer program for speciation, batch-reaction, one-dimensional transport, and inverse geochemical calculations, U.S. Geological Survey Techniques and Methods, book 6, chap. A43, 497 pp., available only at http://pubs.usgs.gov/tm/06/a43/.

Peng, G., Jiao, W.Q., Li, D.M., Li, G.Y., 1981. Division and correlation of the late Quaternary stratigraphy and discussion on the recent tectonic movement in the region of the Luanhe River Delta. Seismoloqy and Geology, 3, 31-36 (in Chinese with English abstract).

Pearson, F.J. and Hanshaw, B.B., 1970. Sources of dissolved carbonate species ingroundwater and their effects on carbon-14 dating. In: IAEA (Ed.), Isotope Hydrology, IAEA, Vienna.

Post, V. E. and Kooi, H., 2003. Rates of salinization by free convection in high-permeability sediments: insight from numerical modeling and application to Dutch coastal area. Hydrogeology Journal, 11, 549-559, doi: 10.1007/s10040-003-0271-7.

Qi, H., Ma, C., He, Z., et al. Lithium and its isotopes as tracers of groundwater salinization, 2019. A study in the southern coastal plain of Laizhou Bay, China. Science of The Total Environment, 650:878-890, doi: 10.1016/j.scitotenv.2018.09.122.

Reilly, T. E. and Goodman, A. S., 1985. Quantitative analysis of saltwater-freshwater relationships in groundwater systems-a historical perspective. Journal of Hydrology, 80, 125-160, doi: 10.1016/0022-1694(85)90078-2.

~~Saito, Y., Katayama, H., Ikehara, K., et al., 1998. Transgressive and highstand systems tracts and post-glacial transgression, the East China Sea. Sedimentary Geology, 122 (1-4), 217-232, doi: 10.1016/S0037-0738(98)00107-9.~~

Sanford, W.E., 2010. Groundwater hydrology: Coastal flow. Nature Geoscience, 3, 671-672, doi: 10.1038/ngeo958.

Santucci, L., Carol, E., Kruse E., 2016. Identification of palaeo-seawater intrusion in groundwater using minor ions in a semi-confined aquifer of the Río de la Plata littoral (Argentina). Science of the Total Environment, 566-567, 1640-1648, doi: 10.1016/j.scitotenv.2016.06.066.

Small, C. and Nicholls, R. J., 2003. A global analysis of human settlement in coastal zones. Journal of Coastal Research. 19, 584-599, doi: 10.2307/4299200.

Sola F., Vallejos A., Daniele L., Pulido-Bosch A., 2014. Identification of a Holocene aquifer-lagoon system using hydrogeochemical data. Quaternary Research, 82,121-131, doi: 10.1016/j.yqres.2014.04.012.

~~Stanley, D.J. and Warne, A.G., 1994. Worldwide Initiation of Holocene Marine Deltas by Deceleration of Sea-Level Rise. Science, 265 (5169), 228-231, doi: 10.1126/science.265.5169.228.~~

Stumpp, C., Ekdal, A., Gonenc, I.E. et al., 2014. Hydrological dynamics of water sources in a Mediterranean lagoon. Hydrology and Earth System Sciences, 18(12):4825-4837, doi: 10.5194/hess-18-4825-2014.

~~Tran, L.T., et al., 2012. Origin and extent of fresh groundwater, salty paleowaters and recent saltwater intrusions in Red River flood plain aquifers, Vietnam. Hydrogeology Journal, 20 (7), 1295-1313, doi: 10.1007/s10040-012-0874-y.~~

Tran, D.A., Tsujimura M., Vo L.P., Nguyen V.T., Kambuku D., Dang T.D., 2020. Hydrogeochemical characteristics of a multi-layered coastal aquifer system in the Mekong Delta, Vietnam. Environmental Geochemistry and Health, 42, 661-680, doi: 10.1007/s10653-019-00400-9.

UN Atlas, 2010. 44 Percent of us Live in Coastal Areas, available at: http://coastalchallenges.com/2010/01/31/un-atlas-60-of-us-live-in-the-coastal-areas.

Vallejos A., Sola F., Yechieli Y., Pulido Bosch A., 2018. Influence of the paleogeographic evolution on the groundwater salinity in a coastal aquifer. Cabo de Gata aquifer, SE Spain. Journal of Hydrology, 557,55-66, doi:

10.1016/j.jhydrol.2017.12.027.

van Engelen J., Oude Essink, Gualbert H.P., Kooi H., Bierkens Marc F.P., 2018. On the origins of hypersaline groundwater in the Nile Delta aquifer. Journal of Hydrology, 560, 301-317, doi: 10.1016/j.jhydrol.2018.03.029.

van Engelen J., Verkaik J., King J., Nofal E.R., Bierkens M.F.P., Oude Essink G.H.P., 2019. A three-dimensional palaeohydrogeological reconstruction of the groundwater salinity distribution in the Nile Delta Aquifer. Hydrology and Earth System Sciences, 23, 5175-5198, doi: 10.5194/hess-23-5175-2019.

Wang, P.X., Min, Q.B., Bian, Y.H. et. al., 1981. Strata of Quaternary transgressions in east China: A preliminary study. Acta Geologica Sinica, 1981 (01), 1-13 (in Chinese with English abstract).

Wang, Y. and Jiao, J.J., 2012. Origin of groundwater salinity and hydrogeochemical processes in the confined Quaternary aquifer of the Pearl River Delta, China. Journal of Hydrology, 438-439, 112-124, doi: 10.1016/j.jhydrol.2012.03.008.

Wang, Y., Fu, G., Zhang, Y., 2010. River-sea interactive sedimentation and plain morphological evolution. Quaternary Science, 27, 674-689, doi: 10.3321/j.issn:1001-7410.2007.05.009, 2007 (in Chinese with English abstract).

Werner, A. D.: A review of seawater intrusion and its managementin Australia, Hydrogeology Journal, 18, 281-285, doi: 10.1007/s10040-009-0465-8.

Werner, A. D., Bakker, M., Post, V. E. A., Vandenbohede, A., Lu, C., Ataie-Ashtiani, B., Simmons, C. T., and Barry, D. A, 2013. Seawater intrusion processes, investigation and management: Recent advances and future challenges. Advance in Water

Resources., 51, 3-26, doi:10.1016/j.advwatres.2012.03.004.
Xu, Q.M., Yuan, G.B., Zhang, J.Q., et al., 2011. Stratigraphic division of the Late Quaternary strata along the coast of Bohai bay and its geology significance. Acta Geologica Sinica, 85 (8), 1352-1367, doi: CNKI:11-1951/P.20110804.1239.004 (in Chinese with English abstract).
Xu, Q.M., Yang, J.L., Yuan, G.B., Chu, Z.X., Zhang, Z.K., 2015. Stratigraphic sequence and episodes of the ancient Huanghe Delta along the southwestern Bohai Bay since the LGM. Marine Geology, 367, 69-82, doi: 10.1016/j.margeo.2015.05.008.
Xu, Q.M., Yang, J.L., Hu, Y.Z., Yuan, G.B., Deng, C.L., 2018. Magnetostratigraphy of two deep boreholes in the southwestern BohaiBay: its tectonic implications and constraints on ages of volcanic layers. Quaternary Geochronology, 43, 102-114, doi: 10.1016/j.quageo.2017.08.006.
Xu, Q.M., Meng, L.S., Yuan, G.B., et al., 2020. Transgressive wave-and tide-dominated barrier-lagoon system and sea-level rise since 8.2 ka recorded in sediments in northern Bohai Bay, China. Geomorphology 352, 106978, doi: 10.1016/j.geomorph.2019.106978.
Xue, C.T., 2009. Historical changes of coastlines on west and south coasts of Bohai Sea since 7000 a B.P.. Scientia Geographic Sinica, 29, 217-222, doi: 10.3969/j.issn.1000-0690.2009.02.012 (in Chinese with English abstract).
Xue, C.T., 2014. Missing evidence for stepwise postglacial sea level rise and an approach to more precise determination of former sea levels on East China Sea Shelf. Marine Geology, 348, 52-62, doi: 10.1016/j.margeo.2013.12.004.

Xue, C.T., 2016. Extents, type and evolution of Luanhe River fan-delta system, China. Marine Geology & Quaternary Geology, 36 (06), 13-22, doi: CNKI:SUN:HYDZ.0.2016-06-004 (in Chinese with English abstract).

Zhou, X., 2013. Basic characteristics and resource classification of subsurface brines in deep-seated aquifers. Hydrogeology & Engineering Geology, 40 (5), 4-10, doi: CNKI:SUN:SWDG.0.2013-05-004 (in Chinese with English abstract).

~~Zong, Y.Q., 2004. Mid-Holocene sea-level highstand along the Southeast Coast of China. Quaternary International, 117, 55-67, doi: 10.1016/S1040-6182(03)00116-2.~~